addition (that is regeneration by oxygen) is assured. A very important means for adjusting the metal-oxygen bond energy of an oxide is by reacting it with another material to produce a new structure with modified bond energies and surface geometry (such as a series of vanadate compounds starting with the alkali vanadates and perhaps ending with heteropoly vanadic acids).

The experimental results described here are consistent with the proposed hypothesis, but there are obvious complicating factors. For example oxygen diffusion from bulk to surface and the reverse process tend to distort somewhat the site distributions of the surfaces from those described in the models. Also phase boundaries, dislocations, and other forms of surface disorder add further complications to the case of real surfaces. However in spite of these complications there is a clearly distinguishable correlation between the approximate surface configuration as described by the model and the selectivity factor in the oxidation of propylene to acrolein.

ACKNOWLEDGMENT

The authors wish to acknowledge The Standard Oil Company (Ohio) for permission to publish this work.

LITERATURE CITED

1. Hearne, G. W., and M. L. Adams, (to Shell Development Co.) *U.S. 2,451,485* (Oct. 19, 1948).
2. Callahan, J. L., R. W. Foreman, and F. Veatch, [to Standard Oil Co. (Ohio)], *U.S. 2,941,007* (June 14, 1960).
3. Twigg, G. H., *Proc. Royal Soc. (London)*, A188, 92 (1946).
4. ———, *Trans, Faraday Soc.*, 42, 284 (1946).
5. Mars, J., and D. W. Van Krevelen, *Chem. Eng. Sci.*, **3**, Spec. Suppl., 41 (1954).
6. Simard, G. L., J. F. Steger, R. J. Arnott, and L. A. Siegel, *Ind. Eng. Chem.*, **47**, 1424 (1955).
7. D'Allessandro, A. F., and A. Farkas, *J. Colloid Sci.*, **11**, 653 (1956).
8. Sittig, M., *Petrol. Refiner*, **40**, No. 11, p. 309 (1961).
9. Kernos, Y. D., and B. L. Moldavskii, *Zhurnol Prikladnoi Khimii*, 33, No. 11, p. 2593 (1960).
10. Veatch, F., J. L. Callahan, E. C. Milberger, and R. W. Foreman, "Catalytic Oxidation of Propylene to Acrolein," Actes du Deuxieme Congres International De Catalyse, Paris 1960, Additions Technip 1961, Paris, Part II, 2647.
11. Foreman, R. W., J. L. Callahan, and F. Veatch, [to the Standard Oil Co. (Ohio)], *U.S. 2,874,191* (Feb. 17, 1959).
12. Voge, H. H., and C. R. Adams (to the Shell Oil Co.), *U.S. 2,991,321* (July 4, 1961).
13. Bretton, R. H., S. W. Wan, and B. F. Dodge, *Ind. Eng. Chem.*, **44**, 594 (1952).
14. Popova, N. I., and V. P. Latyshev, *Dokl. Akad. Nauk SSSR*, **147**, 1382 (1962).
15. Fisher, R. A., and F. Yates, "Statistical Tables for Biological, Agricultural and Medical Research," Hafner Publishing Co., Inc., New York (1949).
16. Kokes, R. J., H. Tobin, Jr., and P. H. Emmett, *J. Am. Chem. Soc.*, **77**, 5860 (1955).
17. Anderson, R. B., K. C. Stein, J. J. Feenan, and L. J. E. Hofer, *Ind. Eng. Chem.*, **53**, 809 (1961).
18. Unpublished data of the Standard Oil Co. (Ohio) Research Laboratory.

Manuscript received December 10, 1962; revision received May 8, 1963; paper accepted June 5, 1963. Paper presented at A.I.Ch.E. New Orleans meeting.

Unsteady State Absorption of Carbon Dioxide by Dilute Sodium Hydroxide Solutions

T. R. REHM, A. J. MOLL, and A. L. BABB
University of Washington, Seattle, Washington

Rates of carbon dioxide absorption by 0.01, 0.05, and 0.1 molar sodium hydroxide solutions were measured at 25°C. for exposure times from 1.4 to 21.6 milliseconds with a laminar-jet technique. Absorption rates were calculated with a model based on one-dimensional diffusion occurring simultaneously with two consecutive irreversible chemical reactions. The resulting partial differential equations were solved with an IBM-709 computer. The calculated absorption rates agreed within 5% of the experimental values.

This work is part of an extensive study of the equilibrium, kinetics, and mass transfer characteristics of the system defined by the overall reaction

$$NaHS + CO_2 + H_2O \rightleftharpoons H_2S + NaHCO_3 \qquad (1)$$

The vapor-liquid equilibrium properties of this system have been reported previously (*18*) as have the reaction kinetics of the individual reactions which together give reaction (1) (*14, 15*). This study was concerned primarily with the unsteady state absorption of carbon dioxide by alkaline solutions. The following reactions were considered:

$$CO_2 + H_2O \underset{k_{r2}}{\overset{k_{f2}}{\rightleftharpoons}} HCO_3^- + H^+ \qquad (2)$$

$$CO_2 + OH^- \underset{k_{r3}}{\overset{k_{f3}}{\rightleftharpoons}} HCO_3^- \qquad (3)$$

T. R. Rehm is with the University of Denver, Denver, Colorado.

$$HCO_3^- + OH^- \underset{k_{r4}}{\overset{k_{f4}}{\rightleftharpoons}} CO_3^= + H_2O \tag{4}$$

$$H^+ + OH^- \underset{k_{r5}}{\overset{k_{f5}}{\rightleftharpoons}} H_2O \tag{5}$$

Several investigators (*5, 19*) derived absorption-rate equations based on the model of absorption with one simultaneous irreversible pseudo first-order reaction:

$$Q = A_i \sqrt{\frac{D_A}{k_{f3}B_o}} \left\{ \left(k_{f3}B_ot + \frac{1}{2} \right) \operatorname{erf} \sqrt{k_{f3}B_ot} + \sqrt{\frac{k_{f3}B_ot}{\pi}} \exp\left(-k_{f3}B_ot\right) \right\} \tag{6}$$

Such a model is valid for this system only if the forward part of reaction (3) is the only reaction which significantly affects the carbon dioxide concentration and if the hydroxyl ion concentration is constant. However, the hydroxyl ion concentration is depleted by reactions (3), (4), and (5). Equation (6), therefore, predicts absorption rates higher than those measured experimentally.

General rate equations have been derived for reaction (3), (*5, 6, 16, 17, 23, 26*) with the assumption of a reversible second-order reaction, but no analytical solution to these equations has been obtained. Perry and Pigford (*25, 26*) numerically solved these rate equations on a computer. Their solutions for the dimensionless instantaneous absorption rate were presented in terms of three other dimensionless parameters:

$$\frac{N}{N_o} = f(k_{f3}B_ot,\ B_o/A_i,\ k_{f3}/k_{r3}) \tag{7}$$

In their numerical solutions the dimensionless diffusivity ratios, D_B/D_A and D_C/D_A, were equal to unity, and their results were limited to values of $k_{f3}B_ot \leqq 5$ and $B_o/A_i =$ 1, 2, and 20.

Brian, Hurley, and Hasseltine (*2*) obtained numerical solutions based on one second-order irreversible reaction. They extended the work of Perry and Pigford by solving for the more elusive dimensionless amount of absorption:

$$\frac{Q}{Q_o} = f(k_{f3}B_ot,\ B_o/A_i,\ D_B/D_A) \tag{8}$$

In addition, they extended the range of parameters to $k_{f3}B_ot = 1{,}000$, $B_o/A_i = 100$, and $0.02 \leqq D_B/D_A \leqq 10$.

In this work a previously suggested model (*12, 17, 23*) was developed for two consecutive irreversible second-order reactions such as the forward parts of reactions (3) and (4). The dimensionless form of the rate equations for this model is equivalent to that of the rate equations based on one reaction with only half the value of B_o. To obtain a more accurate comparison with experimental results for dilute solutions than could be obtained by interpolating the numerical results of Brian, Hurley, and Hasseltine, a computer program was written to solve the applicable differential equations.

The first part of this paper briefly presents the derivation and numerical solution of the rate equations applicable to the unsteady state absorption of carbon dioxide by alkaline solutions. The second part presents the experimental absorption rates measured with a laminar-jet technique. Finally, a comparison between the calculated and the experimental results is made.

Additional experimental data for the absorption of carbon dioxide in alkaline solutions with a laminar-jet technique have been reported (*23, 24*). Since these data are for hydroxyl ion concentrations and contact times outside the range of this study, no comparisons could be made similar to those in Figures 3 to 5.

TABLE 1. FORWARD AND REVERSE REACTION RATE CONSTANTS AT 25°C.

Constant	Value	References
k_{f2} (g.-moles/cc.)$^{-1}$ sec.$^{-1}$	25 - 34	*14, 20, 27, 28*
k_{r2} (g.-moles/cc.)$^{-1}$ sec.$^{-1}$	4×10^7	*14*
k_{f3} (g.-moles/cc.)$^{-1}$ sec.$^{-1}$	8×10^6	*28*
	3×10^{8}*	*14*
k_{r3} sec.$^{-1}$	0.006	*14*
k_{f5} (g.-moles/cc.)$^{-1}$ sec.$^{-1}$	1.3×10^{14}	*11*
k_{r5} sec.$^{-1}$	2.6×10^{-5}	*11*

* This high value may be attributed in part to a proton exchange type of reaction (*8*).

MATHEMATICAL ANALYSIS

Reaction Rate Constants

The values of most of the rate constants in reactions (2) through (5) were determined and are listed in Table 1. Reaction (5), the neutralization reaction, is rapid; the k_{f5} value is the highest value of any second-order rate constant ever measured. Reaction (4), another ionic reaction, also should be rapid since it is equivalent to the dissociation of the bicarbonate ion followed by neutralization of the hydrogen ion formed. Eigen (*11*) determined that the rate constant for the analogous reaction of the dissociation of the bisulfate ion is 10^9 sec.$^{-1}$ Reactions (4) and (5), therefore, are faster than reactions (2) and (3).

The relative values of k_{f2} and k_{f3} show that in the pH range used in this work the amount of carbon dioxide consumed by reaction (2) is small in comparison with that consumed by reaction (3). Furthermore, at pH values above 11 reactions (3) and (4) are essentially irreversible since the equilibrium favors the carbonate ion over the bicarbonate ion. At high pH reaction (5) has a completely negligible effect upon the hydroxyl ion concentration. Therefore, the only reactions that significantly affect the carbon dioxide concentration are the forward parts of reactions (3) and (4). The reaction model, therefore, is of the form

$$A + B \xrightarrow{k_{f3}} C \tag{9}$$

$$B + C \xrightarrow{k_{f4}} \text{Products} \tag{10}$$

Rate Equations

With the above model as a basis, the rate equations describing the absorption of carbon dioxide into a laminar liquid film or jet with simultaneous reaction may be written as

$$\frac{\partial A}{\partial t} = D_A \frac{\partial^2 A}{\partial x^2} - k_{f3}AB \tag{11}$$

$$\frac{\partial B}{\partial t} = D_B \frac{\partial^2 B}{\partial x^2} - k_{f3}AB - k_{f4}BC \tag{12}$$

$$\frac{\partial C}{\partial t} = D_C \frac{\partial^2 C}{\partial x^2} + k_{f3}AB - k_{f4}BC \tag{13}$$

with boundary conditions

$$t = 0,\ x > 0,\ A = 0,\ B = B_o,\ C = 0 \tag{14}$$

$$t \geqq 0,\ x = 0,\ A = A_i,\ \partial B/\partial x = 0,\ \partial C/\partial x = 0 \tag{15}$$

$$t \geqq 0,\ x \to \infty,\ A = 0,\ B = B_o,\ C = 0 \tag{16}$$

where A, B, and C represent the concentrations of carbon dioxide, hydroxyl ion, and bicarbonate ion, respectively. These rate equations and boundary conditions are based upon the following assumptions: the hydroxyl ion concentration at the liquid surface remains high enough so that the reaction model given by reactions (9) and (10) is valid; the diffusion is in only one dimension; the values of D_A, D_B, D_C, k_{f3}, k_{f4}, and A_i are independent of concentration for dilute solutions; there is no gas phase or interfacial resistance to mass transfer; the penetration depth of carbon dioxide is small in comparison to the thickness of the absorbing liquid film or the radius of the absorbing liquid jet; and the velocity of the liquid is constant with exposure time and depth into the liquid.

Since reaction (4) is rapid, there is no appreciable accumulation of C, and its derivatives are small. Equation (13) may then be written as

$$k_{f3}AB = k_{f4}BC \tag{17}$$

When Equation (17) is substituted into Equation (12), one obtains

$$\frac{\partial B}{\partial t} = D_B \frac{\partial^2 B}{\partial x^2} - 2k_{f3}AB \tag{18}$$

Equations (11) and (18) with boundary conditions are sufficient to describe the absorption of A.

These equations may be put into dimensionless form by substituting the dimensionless quantities, a, b, θ, z, r, and q, as

$$\frac{\partial a}{\partial \theta} = \frac{\partial^2 a}{\partial z^2} - ab \tag{19}$$

$$\frac{\partial b}{\partial \theta} = r\frac{\partial^2 b}{\partial z^2} - \frac{2}{q}ab \tag{20}$$

with boundary conditions

$$\theta = 0, z > 0, a = 0, b = 1 \tag{21}$$

$$\theta \geqq 0, z = 0, a = 1, \partial b/\partial z = 0 \tag{22}$$

$$\theta \geqq 0, z \rightarrow \infty, a = 0, b = 1 \tag{23}$$

These equations are of the same form as those of Brian, Hurley, and Hasseltine (*2*). Their numerical solutions, however, cannot be interpolated accurately to compare with the experimental results obtained in this work, and therefore a new series of numerical solutions was calculated.

Numerical Method

Equations (19) and (20) were solved numerically with an explicit iterative finite difference method over a rectangular grid of the type described by Crandall (*3*). The derivatives in Equations (19) and (20) were approximated by the difference equations used by Perry (*25*) with one exception. The first derivatives at the interior grid points were approximated by three-point central-difference equations rather than the two-point backward-difference equations used by Perry. The application of boundary conditions and the path of iteration used to calculate the values of $a(i, j)$ and $b(i, j)$ across the grid were the same as those used by Perry.

After each iteration the instantaneous absorption rate of component A was calculated for each increment of θ from the Fick's law equation:

$$N = -D_A\,(\partial A/\partial x)_{x=0} = -A_i\sqrt{k_{f3}B_oD_C}\,(\partial a/\partial z)_{z=0} \tag{24}$$

A five-point numerical approximation given by Milne (*21*) was used to approximate $(\partial a/\partial z)_{z=0}$ and resulted in the expression

$$N(i) = \frac{A_i\sqrt{k_{f3}B_oD_A}}{12\Delta x}\{25a(i, 1) - 48a(i, 2) + 36a(i, 3) - 16a(i, 4) + 3a(i, 5)\} \tag{25}$$

The values of Q, the total amount of absorption defined by

$$Q = \int_0^t N dt \tag{26}$$

were calculated with Simpson's rule to integrate numerically the N vs. t curves.

The accuracy of the numerical solutions was insured by two general methods: extrapolation of numerical parameters and use of limiting analytical solutions for simplified models. The first method included extrapolating to zero grid spacing ($\Delta\theta \rightarrow 0$, $\Delta z \rightarrow 0$ with $\Delta\theta/(\Delta z)^2$ = constant), to zero reciprocal film thickness $\left(\frac{1}{n\Delta z} \rightarrow 0\right)$, and to an infinite number of iterations. The effect of the two latter extrapolations was less than 1% and therefore was ignored. The extrapolation to zero grid spacing resulted in Q values not more than 2% different than those obtained at the smallest grid spacings. The second method was used to evaluate Q at low values of θ where Q must approach the pseudo first-order value given by Equation (6). Also, the value of Q must not be less than the value given by the physical-absorption model nor greater than the value given by the infinitely fast second-order model (*2, 36*). The numerical solutions in this work never violated either of these last two conditions.

This numerical solution was programmed in FORTRAN language for the IBM-709 computer. The machine time, 7 min. to run 175 iterations over a 37-by-31 grid, was not excessive. A description of the computer program is given elsewhere (*22*).

EXPERIMENTAL METHOD

Apparatus

The laminar-jet technique used in this work is similar in principle to that used by others (*4, 10, 19, 33, 37*). Raimondi and Toor (*29*) and Harvey and Smith (*13*) have shown that there is negligible interfacial resistance in the absorption of carbon dioxide into water.

The absorption chamber was constructed from a 45 to 50 standard taper ground-glass joint (Figure 1) fitted with a receiver receptacle, a liquid outlet, two gas ports, a thermometer

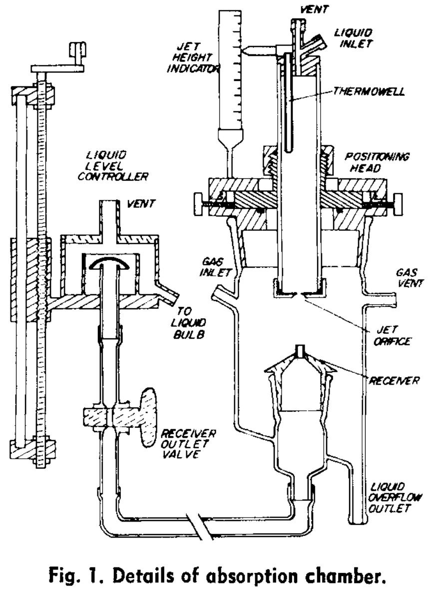

Fig. 1. Details of absorption chamber.

holder, and a liquid-overflow drain at the lower end of the sloped bottom. The holder for the jet-forming column was an adjustable brass bushing placed in a tapered brass ring fitted to the top of the 45 to 50 ground-glass joint. The length of the exposed liquid jet was varied by sliding the jet-forming column up or down through the positioning head. The jet length was measured by a scale attached to the positioning head. The jet-forming element was a thin brass orifice plate 6 mils thick with a hole diameter of 0.140 cm. The calming section above the orifice plate was necessary to assure that the liquid was not disrupted into turbulent eddies that would disturb the laminar characteristic of the exposed jet.

The orificed jet was used in preference to the jet formed from a long small-diameter tube since the latter does not attain plug flow characteristics until it is some appreciable distance below the outlet (*4, 32, 34*). In addition, a thin plate orifice was chosen because it is easier to construct than a thick shaped orifice where it is difficult to attain the mathematically desired curvature of the orifice inlet. An analysis of photographs of the jet formed from a 0.140-cm. orifice showed that a constant diameter of 0.119 ± 0.002 cm. was attained in a distance of less than 3 diam. from the orifice. This diameter reduction of 15% is less than the accepted value of 22% probably because of viscous effects. The first section of the jet, equivalent to 3 jet diam., was not visible in the photograph owing to the presence of the orifice holder. However, a theoretical analysis (*1*) showed that most diameter reduction should occur in a distance of 1 jet diam.

The jet receiver was designed to collect the entire jet of liquid without gas entrainment. The jet formed by a 0.140-cm. diam. orifice was collected perfectly in a short section of 0.170-cm. I.D. glass tubing. This tube provided a short smooth sharp-edged receiving element for the larger receiver vessel. The liquid level in the receiver element was controlled by a liquid-level controller on the outlet liquid stream. A considerable head of liquid was needed between the receiver and controller to counteract the velocity head of the entering jet. This head varied with liquid-flow rate but was approximately 25 cm. With this arrangement, the jet length, alignment, and receiver condition could be controlled precisely.

To measure the gas- and liquid-flow rates a displacement technique was developed in which the electrical conductance of the displacing liquid was used to trigger a timer automatically. Mercury was used to displace the gas from the gas bulb. A similar arrangement also was used for the liquid-flow rate since the liquid would be sufficiently conductive after exposure to the gas. A dual-channel electronic flow-rate detector was designed and constructed (*30*) which would start a timer when the level reached a certain mark in a calibrated vessel and then shut it off at a second mark. When connected to a precision timer this automatic flow-rate detector provided time measurements reproducible to within ± 0.3%. Details of the technique are given elsewhere (*30*).

The exposure times of the liquid to the gas could be varied by changing the liquid-flow rate, the jet diameter, and the jet length. In this work the jet diameter was kept constant at 0.119 cm., and liquid-flow rates of 3.0 and 4.5 cc./sec. were used with jet lengths from 0.84 to 8.02 cm. This combination of conditions resulted in a range of exposure times from 1.4 to 21.6 milliseconds.

Procedure

The various steps in the experimental procedure to obtain the absorption rates of carbon dioxide into sodium hydroxide solutions are summarized below, but more detailed procedures are listed elsewhere (*30*).

The constant-temperature bath was filled with water and its temperature adjusted to maintain a temperature of 25.0 ± 0.05°C. in the absorption chamber. After temperature equilibrium was obtained, the desired jet length was set by raising or lowering the jet-forming column. Gas flow through the chamber was then started and allowed to continue for approximately 15 min. to displace all the air from the system. Then the gas was saturated with water vapor by passage through the gas bubbler. The level of the mercury in the gas bulb was then raised to just below the lower probe. As the liquid absorbed carbon dioxide from the absorption chamber, the drop in chamber pressure was counteracted by raising the leveling bulb and, thus, the mercury level in the gas bulb. Moreover, as the absorption continued at constant pressure, the mercury level rose in the gas bulb first completing the timer start-circuit and then the timer stop-circuit. After the run was completed, the gas system was opened to the gas supply and the absorption chamber and the gas bulb flushed with dry carbon dioxide. The liquid-flow rate was determined by diverting the liquid stream into the liquid flow-rate bulb where the time required to fill the calibrated bulb was measured. This overall procedure was repeated for several different jet lengths.

The carbon dioxide used was a commercial grade and 99.975% pure. Reagent-grade sodium hydroxide, low in carbonate, was used to prepare carbonate-free sodium hydroxide solutions. Chemical analysis of these solutions indicated a negligible concentration of carbonate ion. The concentration of the sodium hydroxide solutions was determined by titration with standard acid.

The distilled water was not degassed in view of both the reproducibility of the data and the good agreement with accepted values of carbon dioxide solubility (*35*) and diffusivity (*9*) obtained for the absorption rates of carbon dioxide in pure water.

RESULTS

Experimental

Figures 2 to 5 present a comparison of experimental absorption rates of carbon dioxide with values predicted with various mathematical models. Figure 2 shows the comparison for absorption into pure water, and Figures 3 to 5 show the comparisons for absorption into 0.01 molar, 0.05 molar, and 0.1 molar sodium hydroxide solutions. Experimental amounts of absorption were calculated at different contact times from the measured values of the jet diameter, d; the jet height, h; the volumetric liquid flow rate, L; and the volumetric gas flow rate, G. The contact time, t, was obtained from the relation

$$t = \frac{\text{jet height}}{\text{jet velocity}} = \frac{\pi d^2 h}{4L} \tag{27}$$

From Equation (26) and the mean value theorem, the amount of absorption, Q was given by

$$Q = N_{\text{avg}}\, t \tag{28}$$

N_{avg} was obtained from the relation

$$N_{\text{avg}} = \frac{\text{volumetric gas flow rate}}{\text{molar volume of gas} \times \text{jet area}} = \frac{G}{v(\pi\, dh)} \tag{29}$$

The molar volume corresponded to that of carbon dioxide completely saturated with water vapor at 25°C. Equations (27) and (29) may be combined to give

$$Q = \frac{Gd}{4vL} \tag{30}$$

The factor, L, which appears in Equations (27) and (30), was varied only between 3.0 and 4.5 cc./sec. and had little effect upon the scatter of the data points on the Q vs. t plots.

Predicted

The theoretical models used to calculate the predicted Q vs. t curves shown in Figures 2 to 5 include purely physical absorption, absorption with pseudo first-order reaction, and absorption with two consecutive second-order reactions. The curves based on purely physical absorption were calculated from the well-known solution to the diffusion equation with semi-infinite boundary conditions:

$$Q_o = 2A\sqrt{\frac{D_A t}{\pi}} \tag{31}$$

The Q vs. t curves in Figures 3 to 5 based upon a pseudo first-order reaction, were calculated from Equation (6). The

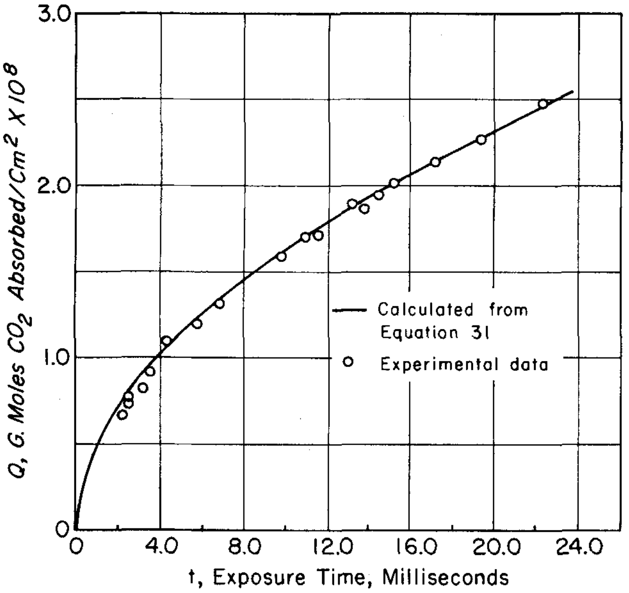

Fig. 2. Integral absorption rates of carbon dioxide into water at 25°C.

amounts of absorption based upon the second-order, two-reaction model described by Equations (11) and (18) were computed with the numerical method described above. In addition, the values of ϕ_a, the dimensionless amount of absorption for the two rapid-reactions model, were calculated from the parametric equations (*2*)

$$\phi_a = \frac{Q}{Q_o} = \frac{1}{\text{erf}\,(\sigma)} \qquad (32)$$

$$q'\sqrt{r} = \frac{q}{2}\sqrt{r} = \frac{1 - \text{erf}\,(\sigma/\sqrt{r})}{\text{erf}\,(\sigma)\,\exp\left\{\sigma^2\left(\frac{r-1}{r}\right)\right\}} \qquad (33)$$

Discussion of Results

Figure 2 shows the agreement between the experimental amount of absorption of carbon dioxide by pure water and values calculated from Equation (31). This agreement confirms some of the previously made assumptions: the diffusion is one-dimensional and there is negligible gas-phase or interfacial resistance to mass transfer, small carbon dioxide penetration depth, and negligible velocity gradients within the jet.

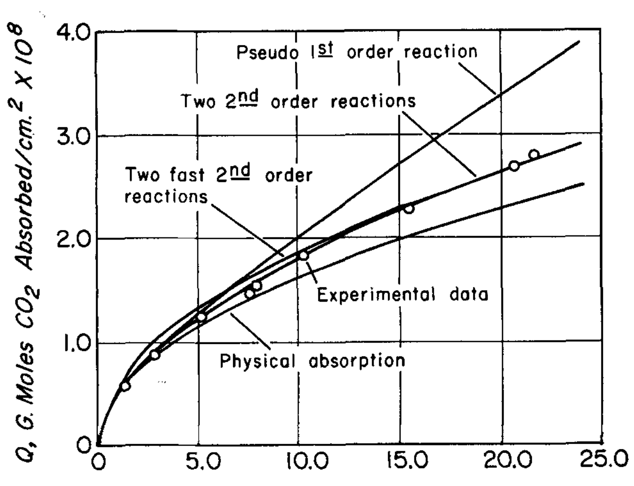

Fig. 3. Integral absorption rates of carbon dioxide by 0.01 molar sodium hydroxide solutions at 25°C. (ϕ_a = 1.16).

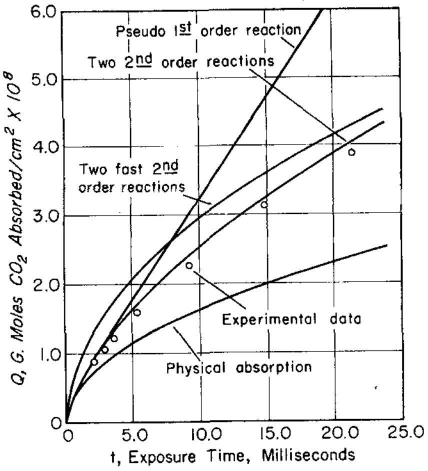

Fig. 4. Integral absorption rates of carbon dioxide by 0.05 molar sodium hydroxide solutions at 25°C. (ϕ_a = 1.80).

The results shown in Figures 3 to 5 indicate that the model of absorption with two consecutive second-order reactions describes the absorption of carbon dioxide into dilute sodium hydroxide solutions better than any of the more simplified models. The agreement between experimental values and numerically computed values of Q in Figure 3 is almost exact. In Figures 4 and 5 the experimental values are shown to agree with the computed values within 5% for most of the data points.

The fact that the experimental data points in Figures 4 and 5 are lower than the computed curves may be explained by the choice of values for the physical properties used in the numerical solutions. In all calculations the values of D_A and A_i were 1.92 × 10^{-5} sq. cm./sec. (*9*) and 3.29 × 10^{-5} g.-moles/cc. (*35*), respectively, the same values as for pure water. For 0.1 molar sodium hydroxide the values of each of these parameters could be decreased by as much as 2% based on empirical correlations. The value used for k_{f3}, shown in Table 1, was obtained by Pinsent and Roughton (*28*). Although D_A, A_i, and k_{f3} are known, estimates of the D_B value vary. The value of 2.3 × 10^{-5} sq. cm./sec. used for D_B was based upon experimental work by Danckwerts and co-workers (*7, 31*). The computed values of Q in Figures 3 to 5 are somewhat insensitive to changes in D_B. Over the range

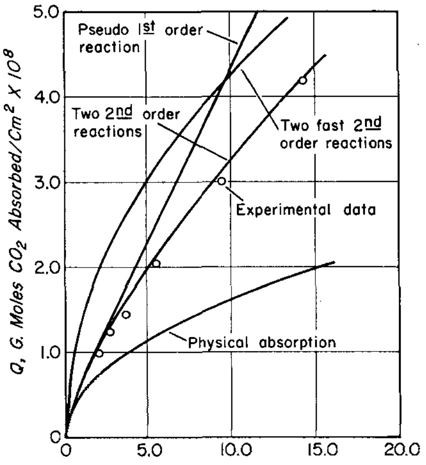

Fig. 5. Integral absorption rates of carbon dioxide by 0.1 molar sodium hydroxide solutions at 25°C. (ϕ_a = 2.61).

$2.0\text{-}3.0 \times 10^{-5}$ sq. cm./sec., the maximum variation in Q was 5%.

Therefore, the unsteady state absorption rates of carbon dioxide into dilute sodium hydroxide solutions agree well with those predicted from a model based on two consecutive second-order reactions without empirical adjustment of A_i, k_{f3}, and D_A.

ACKNOWLEDGMENT

The authors are grateful to the National Science Foundation for financial support of this work.

NOTATION

A = concentration of carbon dioxide at a particular point in the absorbing liquid, g.-moles/cc.
A_i = concentration of carbon dioxide at liquid interface, assumed to be the solubility of carbon dioxide in water, g.-moles/cc.
a = A/A_i, dimensionless concentration of carbon dioxide
B = concentration of hydroxyl ion at a particular point in the liquid, g.-moles/cc.
B_o = initial concentration of hydroxyl ion, g.moles/cc.
b = B/B_o, dimensionless concentration of hydroxyl ion
C = concentration of bicarbonate ion at a particular point in the liquid, g.-moles/cc.
D_A = diffusion coefficient of carbon dioxide in liquid, sq. cm./sec.
D_B = diffusion coefficient of hydroxyl ion, sq. cm./sec.
D_c = diffusion coefficient of bicarbonate ion, sq.cm./sec.
d = diameter of jet, cm.
$\text{erf}(x) = \dfrac{2}{\sqrt{\pi}} \displaystyle\int_0^x e^{-x^2}\, dx$
f = functional notation
G = volumetric gas-flow rate, cc./sec.
h = jet height, cm.
i = index denoting grid point corresponding to a value of $\theta = (i-1)\,\Delta\theta$
j = index denoting grid point corresponding to a value of $z = (j-1)\,\Delta z$
$k_{f2}, k_{r2}, k_{f3}, k_{r3}, k_{f4}, k_{r4}, k_{f5}, k_{r5}$ = forward and reverse reaction-rate constants for reactions (2) through (5), respectively, (g.-moles/cc.)$^{-1}$ sec.$^{-1}$, or sec.$^{-1}$
L = volumetric liquid-flow rate, cc./sec.
n = number of increments of z used in grid
N = instantaneous rate of absorption, g.-moles/sq. cm. sec.
N_o = instantaneous rate of absorption for purely physical absorption g.-moles/sq. cm. sec.
N_{avg} = average rate of absorption over entire surface of jet, g.-moles/sq. cm. sec.
Q = total amount of absorption, g.-moles/sq. cm.
Q_o = total amount of absorption for purely physical absorption, g.-moles/sq. cm.
q = B_o/A_i, dimensionless boundary concentration ratio
q' = $q/2$
r = D_A/D_B, dimensionless diffusivity ratio
t = exposure time, sec.
v = molar volume of carbon dioxide, cc.
x = distance into jet from surface, cm.
$z = \sqrt{\dfrac{k_{f3}B_o}{D_A}}\, x$, dimensionless time

Greek Letters

θ = $k_{f3}B_o t$, dimensionless time
σ = parameter in Equations (32) and (33)
ϕ_a = Q/Q_o, for infinitely fast reactions
Δz = increment size of z used in numerical solution
$\Delta\theta$ = increment size of θ used in numerical solution

LITERATURE CITED

1. Birkhoff, Garrett, and E. H. Zarantonello, "Jets, Wakes, and Cavities," p. 230, Academic Press, New York (1957).
2. Brian, P. L. T., J. F. Hurley, and E. H. Hasseltine, *A.I.Ch.E. Journal*, **7**, 226 (1961).
3. Crandall, S. H., "Engineering Analysis," p. 377, McGraw-Hill, New York (1956).
4. Cullen, E. J., and J. F. Davidson, *Trans. Faraday Soc.*, **53**, 113 (1957).
5. Danckwerts, P. V., *ibid.*, **46**, 300, 701 (1950).
6. ———, *Ind. Eng. Chem.*, **43**, 1460 (1951).
7. ———, and A. M. Kennedy, *Chem. Eng. Sci.*, **8**, 201 (1958).
8. Danckwerts, P. V., and K.-A. Melkerson, *Trans. Faraday Soc.*, **58**, 1832 (1962).
9. Davidson, J. F., and E. J. Cullen, *Trans. Inst. Chem. Engrs. (London)*, **35**, 51 (1957).
10. Edwards, G., R. Robertson, F. Rumford, and J. Thomson, *ibid.*, **32**, S6 (1954).
11. Eigen, Manfred, *Discussions Faraday Soc.*, **17**, 194 (1954).
12. Gilliland, E. R., R. F. Baddour, and P. L. T. Brian, *A.I.Ch.E. Journal*, **4**, 223 (1958).
13. Harvey, E. A., and W. Smith, *Chem. Eng. Sci.*, **10**, 274 (1959).
14. Himmelblau, D. M., and A. L. Babb, *A.I.Ch.E. Journal*, **4**, 143 (1958).
15. ———, *Ind. Eng. Chem.*, **51**, 1403 (1959).
16. Kishinevsky, M. Kh., *J. Appl. Chem. USSR (English Transl.)*, **27**, 415 (1954).
17. Krevelen, D. W. van, and P. J. Hoftijzer, *Rec. Trav. Chim.*, **67**, 563 (1948).
18. Mai, K. L., and A. L. Babb, *Ind. Eng. Chem.*, **47**, 1749 (1955).
19. Matsuyama, Takuzo, *Mem. Fac. Eng. Kyoto Univ.*, **15**, 142 (1953).
20. Mills, G. A., and H. C. Urey, *J. Am. Chem. Soc.*, **62**, 1019 (1940).
21. Milne, W. E., "Numerical Calculus," p. 97, Princeton Univ. Press, Princeton, N. J. (1949).
22. Moll, A. J., M.S. thesis, Univ. Washington, Seattle, Wash. (1961).
23. Nijsing, R. A. T. O., R. N. Hendriksz, and H. Kramers, *Chem. Eng. Sci.*, **10**, 88 (1959).
24. Onda, Kakusabura, Tadayashi Okamoto, and Yukio Yamaji, *Chem. Eng., (Tokyo)*, **24**, 918 (1960).
25. Perry, R. H., Ph.D. thesis, Univ. Delaware, Newark, Del. (1953).
26. ———, and R. L. Pigford, *Ind. Eng. Chem.*, **45**, 1247 (1953).
27. Pinsent, B. R. W., L. Pearson, and F. J. W. Roughton, *Trans. Faraday Soc.*, **52**, 1512 (1956).
28. Pinsent, B. R. W., and F. J. W. Roughton, *ibid.*, **47**, 263 (1951).
29. Raimondi, Pietro, and H. L. Toor, *A.I.Ch.E. Journal*, **5**, 86 (1959).
30. Rehm, T. R., Ph.D. thesis, Univ. Washington, Seattle, Wash. (1960).
31. Roberts, D., and P. V. Danckwerts, *Chem. Eng. Sci.*, **17**, 961 (1962).
32. Scriven, L. E., and R. L. Pigford, *A.I.Ch.E. Journal*, **4**, 382 (1958).
33. *Ibid.*, p. 439.
34. *Ibid.*, **5**, 397 (1959).
35. Seidell, Atherton, "Solubilities of Inorganic and Metal Organic Compounds," p. 460, Van Nostrand, New York (1958).
36. Sherwood, T. K., and R. L. Pigford, "Absorption and Extraction," p. 336, McGraw-Hill, New York (1952).
37. Vielstich, Wolf, *Chem. Ing. Tech.*, **28**, 543 (1956).

Manuscript received August 11, 1962; revision received April 8, 1963; paper accepted April 8, 1963. Paper presented at A.I.Ch.E. Chicago meeting.